FEM-aided design of a novel device for soil anchoring

Conception assistée par éléments finis d’un nouveau système pour l’ancrage des sols

Prisco di C., Pisanò F.
Politecnico di Milano

ABSTRACT: In this paper the pull-out performance of an innovative system for soil anchoring is mechanically interpreted on the basis of a preliminary finite element investigation. The system consists of a tie rod equipped with thick steel sockets, extruding into the soil to increase the overall pull-out bearing capacity. The effectiveness of the anchorage comes from two correlated strength mechanisms: a direct one, associated with the shear/flexural strength of the sockets themselves; and an indirect one, in the form of a remarkable increase in the normal confinement on the tie rod and hence in the available shear strength. Finally, the numerical results are exploited to conceive a design-oriented analytical model for the prediction of the pull-out bearing capacity.

RÉSUMÉ: Dans cette article, le comportement en tension de un nouveau système pour l’ ancrage dans les sols est interprété sur la base de une analyse préliminaire avec les éléments finis. Dans le système il y a une bar en métal avec des puntons qui s’extrudent dans le sol pour augmenter la capacité totale de l’instrument. L’efficience de l’ ancrage dérive de deux mécanismes résistants: un qui peux être définis direct, associe a la résistance des puntons, et un indirect, associe à l’incrément du confinement sur la bar. Les résultats numériques ont été utilisés pour définir un model interprétatif du fonctionnement du system d’ ancrage.
KEYWORDS: soil anchoring, pull-out, soil–structure interaction, finite element analyses, plasticity

1 INTRODUCTION

The analysis and the design of soil anchors are of major interest to geotechnical engineers in many practical applications, including retaining structures, transmission towers, marine pipelines, etc. For these purposes, the employment of the Finite Element Method (FEM) is progressively increasing, as it overcomes the limitations of most empirical/analytical approaches (Das 1990) in dealing with complex geometries and material non-linearities. On the research side, only a few papers present numerical results about soil anchoring systems, compared to the available experimental data and analytical predictions (see for instance Rowe and Davis (1982a,b), Merifield and Sloan (2006)).

This paper summarizes a recent research activity (di Prisco and Pisanò 2012) concerning the study of a novel device for soil anchoring. This latter is formed by a tie rod equipped with thick steel sockets, which are extruded into the soil to ensure a remarkable pull-out capacity.

To investigate the soil—structure interaction (SSI) mechanisms determining the effectiveness of the system, FEM simulations of pull-out tests have been performed. Then, based on the critical analysis of the numerical outcomes, an analytical model for the estimation of the pull-out capacity has been set up. Despite the approximations introduced, the good agreement between analytical and FEM results is believed to represent the starting point for the conception of a reliable design procedure.

2 FEM SIMULATION OF PULL-OUT TESTS

The novel setup of the anchoring device under consideration is characterized by the presence of internal steel sockets along the tie rod shaft, to be extruded - after the rod installation - into the soil by means of a hydraulic system. Recent in situ pull-out tests have highlighted how socket extrusion ensures a very large bearing capacity (Santoro 2009), much larger than in the usual case of grouted anchorages.

Figure 1 sketches the installation of the anchoring system, composed of the tie rod and the extruded steel sockets, while Figure 2 illustrates the telescopic structure of the sockets. The system is rather flexible in terms of geometrical configuration as the number, the location, and the orientation of the sockets can be freely designed; its installation is extremely fast and inexpensive.

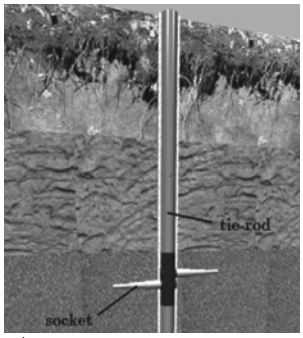

Figure 1. The anchoring system.

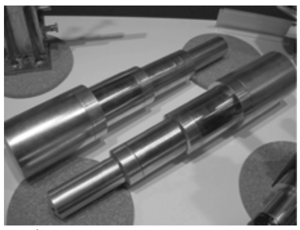
Figure 2. The steel sockets.

2.1 *FEM model*

The geometrical configuration for numerical analyses has been kept as simple as possible, but sufficiently accurate to reproduce the most relevant structural details. If the four sockets were located at the same vertical level (they are not to allow room for the extruding hydraulic circuits), the anchor would be characterized by four (vertical) symmetry planes. Although this is not exactly true, it has been here assumed for computational convenience that the different socket elevations only slightly violate such symmetries: accordingly, only a quarter of the whole geometry has been considered and discretized.

The FEM mesh employed is shown in Figure 3. The discretization – performed by adopting quadratic tetrahedral elements - is finer around the sockets and the tie rod, i.e. where the solution is expected to exhibit the largest gradients. The external soil boundaries have been placed sufficiently far from the anchor, so as to not affect the global pull-out response.

Since the main purpose of this preliminary study was the highlighting of SSI mechanisms, for the sake of simplicity no sophisticated material models have been considered. In particular, the soil mechanical behaviour has been modelled by means of a simple Mohr-Coulomb perfectly-plastic constitutive relationship with non-associated flow rule (i.e. with different friction and dilatancy angles), while a von Mises perfectly-plastic associated model has been adopted for the anchor structural members. A linear variation along the depth has been introduced for the soil Young modulus, to account for the stiffening induced by the increase in normal confinement. Moreover, as is commonly done in SSI analyses, a widthless perfectly-plastic interface layer has been interposed between the anchor and the surrounding soil to allow both shear and tension detachments.

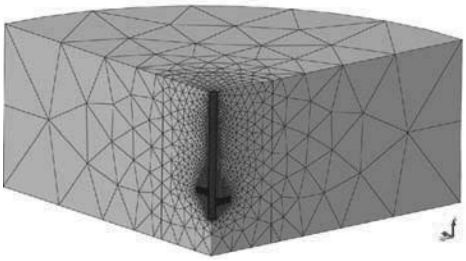

Figure 3. FEM model.

Apparently, the length of the tie rod, i.e., the socket extrusion depth, greatly influences the pull-out capacity of the anchor: as deeper anchors are considered, larger discrete models should be defined, implying an increase in computational costs. Conversely, in order to investigate how the strength contribution coming from the steel sockets is affected by the initial stress state, an approximate approach has been here adopted for the first preliminary analyses. In particular, to simulate a real higher embedment, the same model in Figure 3 has been used for different physical depths, by using an equivalent ``embedment surcharge" q_{emb} on the top of the reduced model (obviously, this assumption neglects the frictional pull-out resistance provided by the missing upper soil).

2.2 *Main inferences from FEM analyses*

In what follows, the main observations derived from the analysis of the preliminary FEM results (with embedment surcharge) are qualitatively summarized.

All the pull-out tests have been performed by imposing a prescribed upward displacement δ at the top of the tie rod, recording the corresponding reaction forces to quantify the global resistance provided by the neighboring soil. While the total pull-out force readily results from the top reaction forces, two distinct contributions can be recognized and estimated on the basis of the FEM outputs. In particular, the global capacity has been split into a first frictional component mobilized along the tie rod, and a second contribution directly carried by the steel sockets.

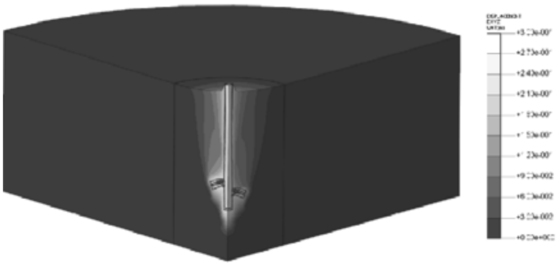

Figure 4. Total displacement contour plot at the onset of failure.

As an example, Figure 4 illustrates the contour plot of the total displacement (absolute value) at the onset of the collapse. The global failure mechanism takes place in the form of a soil wedge surrounding the anchor and moving upward as the anchor itself is pulled-out. Such a failure mechanism is further illustrated in terms of the plastic shear strain in Figure 5: the shear strain concentrations take place along the tie rod and close to the sockets, so that the formation of a failure wedge is apparent.

Figure 5. Plastic shear strain contour plot at the onset of failure.

Figure 6 shows, for four different q_{emb} values, the pull-out curves (force vs. displacement) estimated for the whole anchorage, i.e. four times the force computed for the quarter anchor (this would rigorously hold if the steel sockets were at the same elevation). In all the cases considered, the mechanical response of the anchorage is overall ductile and the limit pull-out load (horizontal plateau) is achieved after quite large displacements. Besides the expected increase in the bearing capacity at larger q_{emb}, it is also worth noting that, owing to the aforementioned spatial variation of the soil Young modulus, the limit load is achieved at about the same displacement level δ.

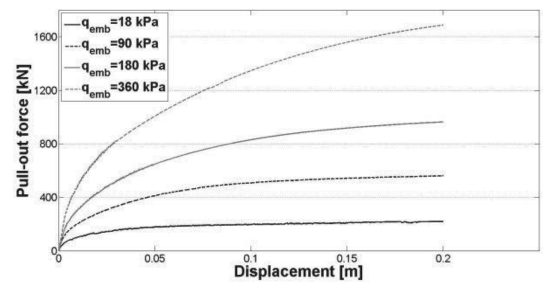

Figure 6. Pull-out responses at increasing embedment surcharge.

Both the above frictional and socket strength contributions have been separately evaluated for all the FEM analyses performed. The obtained values – not reported here for the sake of brevity – show that the lateral frictional forces and the contribution provided by the steel sockets are quantitatively comparable. Such large lateral forces could not be explained by assuming a standard k_0 distribution for the confining stress (k_0 stands for the at rest earth pressure coefficient) all around the tie rod. In contrast, the numerical simulation shows a significant increase in confining stresses as the anchor is pulled-out, up to values much larger than the at rest ones. Figure 7 illustrates the final contour plot of the radial stress, in which the severe perturbation of the initial (linear) at rest distribution is evident.

In the light of these considerations, the influence of the steel sockets on the global pull-out capacity can be said to be twofold. First, the sockets directly sustain a portion F_{socket} of the external load owing to their shear/flexural strength: henceforth, this will be referred to as the "direct effect". Besides this, an "indirect effect" stems from the formation of a global failure mechanism with a remarkable increase in the radial stress around the tie rod and, therefore, in the mobilizable shear force $F_{lateral}$. For any future design purpose, the necessity of a reliable estimation of both F_{socket} and $F_{lateral}$ is self-evident.

Figure 7. Radial stress contour plot at the onset of failure.

3 A DESIGN-ORIENTED ANALYTICAL MODEL

In this section a design-oriented analytical model is defined to estimate each resisting component contributing to the total pull-out capacity of the anchor. The accuracy of the model has been also assessed by comparing the analytical results with the outcomes from full-size FEM analyses, i.e. with no embedment surcharge.

Apparently, the near presence of the tie rod prevents the sockets from being interpreted as isolated deeply buried pipes, so that the force exerted by the soil on each socket (and viceversa) cannot be evaluated via the well-known concept of ``uplift coefficient" (or even ``break-out coefficient" - see for instance, Rowe and Davis (1982a,b), Merifield and Sloan (2006), White *et al.* (2008). In contrast, it has been numerically observed that the soil between a single socket and the tie rod behaves as if it was rigidly connected to the anchor, giving rise to a sort of ``corkscrew mechanism".

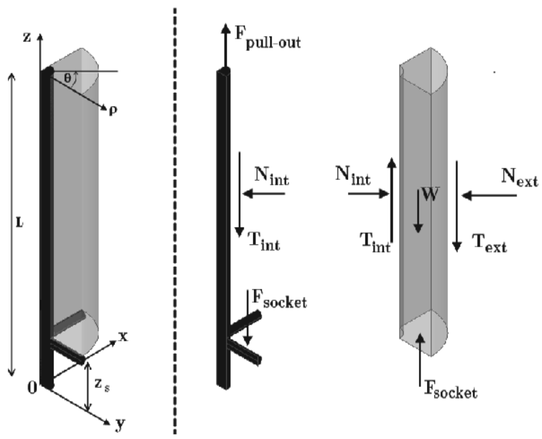

Figure 8. Simplified static scheme for the anchoring system.

To evaluate at the same time both F_{socket} and $F_{lateral}$, the simplified vertical wedge mechanism in Figure 7 (left picture) is considered (the shear force T_{int} coincides with $F_{lateral}$). For the sake of simplicity, the two half-sockets are assumed to be positioned at the same elevation, so that a cylindrical reference frame (ρ,θ,z) can be setup to describe an axisymmetric stress/strain state within the soil wedge (axisymmetric conditions are indeed expected beyond a given distance over the sockets). The right picture in Figure 8 illustrates the reference static scheme, i.e. the forces acting both on the tie rod and the soil wedge (the rod weight is neglected and boundary reaction forces are not visualized).

From the analysis of all numerical results the following conclusions have been drawn:

1. except for local disturbances next to the sockets, all the stress components are almost linearly distributed along the vertical z-axis;
2. the vertical direct strain component ε_z is much less than the other two (ε_ρ and ε_θ), so that $\varepsilon_z = 0$ can be assumed;
3. the normal force N_{ext} in Figure 8 can be approximately evaluated by assuming a k_P linear distribution for the radial stress σ_r along the outer side of the soil wedge (k_P stands for the passive earth pressure coefficient);
4. the inner and the outer σ_r distributions can be linearly related through a dimensionless constant λ;
5. the failure distributions of the mobilized friction angle $\phi_{mob} = \arctan\left(\tau_{z\rho} / \sigma_\rho\right)$ along the inner and outer sides of the soil wedge exhibit a mean value less than the soil friction angle ϕ and approximately equal to:

$$\tan\phi_{mob}^{\lim} = \frac{\cos\phi\cos\psi}{1-\sin\phi\sin\psi} \qquad (1)$$

where ψ is the soil dilatancy angle.

Relationship (1) stems from the fact that, during the pull-out process, the aforementioned soil wedge undergoes a sort of ``axisymmetric simple shear loading". In other words, the loading conditions of the soil elements around the tie rod are highly constrained and similar to those a soil specimen experiences within a so-called simple shear apparatus: as was recently discussed by di Prisco and Pisanò (2011), this implies the material dilatancy to significantly affect the limit shear stress.

The above considerations lead to the formulation of the following system of equations:

$$\begin{cases} T_{int} + F_{socket} = T_{ext} \\ T_{int} = N_{int}\tan\phi_{mob} \\ T_{ext} = N_{ext}\tan\phi_{mob} \\ N_{int} = \lambda N_{int} \end{cases} \qquad (2)$$

with the unknowns N_{int}, T_{int} ($= F_{lateral}$), T_{ext} and F_{socket} (N_{ext} is simply obtained by integrating the k_P - σ_r distribution along the outer surface of the soil wedge). While the equations in system (2) hold at any stage of the loading process, $\phi_{mob} = \phi_{mob}^{\lim}$ is to be set at failure – i.e. when the limit frictional capacity is attained along the sides of the soil wedge.

For system (2) to be solved, the determination of the coefficient λ introduced in the previous assumption 4 is required. For this purpose, an original procedure has then been conceived: this is based on the solution of a classical rock engineering problem, concerning the determination of the elastic stress state around a circular cavity (Jeager *et al.* 2007). For this purpose, an axisymmetric boundary value problem has been posed by assuming that: (i) the soil wedge in Figure 8 is internally elastic; (ii) the direct strain ε_z is nil; and (iii) the vertical stress gradients are much lower than those along the radial direction. While the problem formulation and the solution strategy can be found in di Prisco and Pisanò (2012), the obtained λ expression is reported here:

$$\lambda = \frac{\pi}{4} R\left(L - z_s\right)\left(\frac{c_1}{2} - \frac{c_2}{2R^2}\right) \qquad (3)$$

where:

$$\begin{cases} c_1 = \dfrac{8(R+l)}{\pi(L-z_s)\left[l^2+2lR+2(1-\nu)R^2\right]} \\ c_2 = \dfrac{8R^2(R+l)(2\nu-1)}{\pi(L-z_s)\left[l^2+2lR+2(1-\nu)R^2\right]} \end{cases} \quad (4)$$

In expressions (3) and (4), R and L are the radius and the length of the tie rod, while l and z_s stand for the length and the elevation (with respect to the bottom of the tie rod) of the steel sockets.

The straightforward solution of system (2) allows of estimating both F_{socket} and T_{int} ($= F_{lateral}$). The soundness of the above assumptions has been verified for all the performed simulations and, in particular, for the full-size analyses (3 m and 7 m embedment) a satisfactory agreement in terms not only of total pull-out force (errors less than 10%) but also of the single contributions has been found. Further confirmation is given in Figures 9 and 10, where the analytical predictions for the radial (a, circular marked line) and shear (b, square marked line) stresses along the inner side of the soil wedge are compared with the FEM results (black solid line).

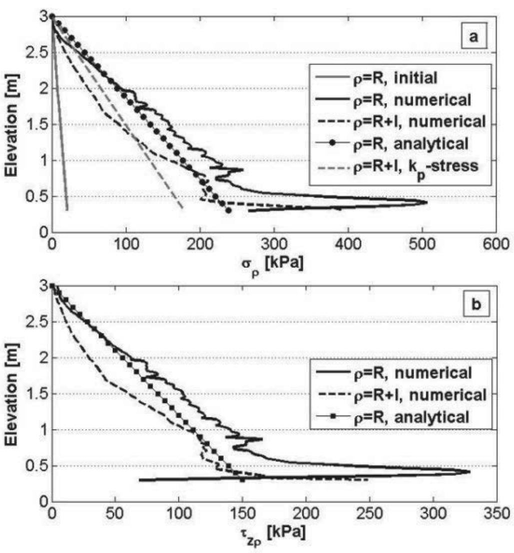

Figure 9. FEM and analytical stress distributions for the full-size model with 3m-embedded sockets.

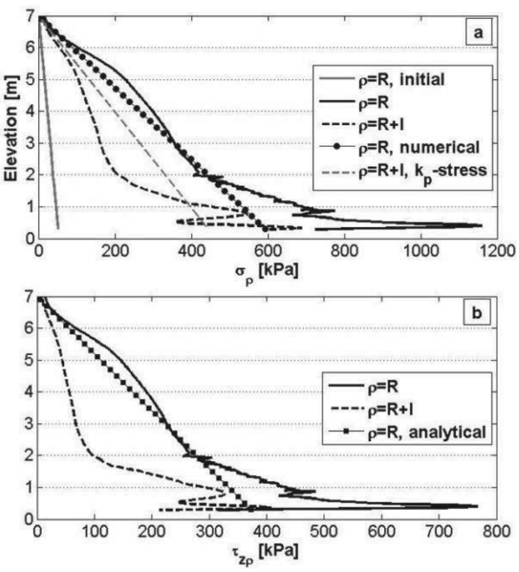

Figure 10. FEM and analytical stress distributions for the full-size model with 7m-embedded sockets.

4 CONCLUSIONS

The pull-out performance of an innovative soil anchoring system has been numerically investigated through FEM analyses. The anchoring device is composed of a tie rod and a set of steel sockets, the latter to be extruded into the soil; former in situ tests have shown the steel sockets largely improve the pull-out performance of the anchorage. The device installation is fast, flexible and inexpensive, while in most cases additional soil grouting becomes optional.

In this work, vertical pull-out tests have been first simulated to explore the SSI mechanisms determining the pull-out capacity of the device, whence the following conclusions have been drawn:

- the steel sockets contribute to the global pull-out capacity in a twofold manner. In a direct way, they sustain a significant part of the total load owing to their shear/flexural strength; they also provide an indirect contribution, by increasing the lateral confinement and the mobilizable friction along the tie rod;
- in all the cases considered, failure develops up to the free surface through a global mechanism involving a cylindrical vertical soil wedge;
- the pull-out strength increases for deeper anchors. Its dependence on socket depth has been found to be, within the investigated range, almost linear;

A simplified analytical model was then proposed to simultaneously estimate the strength contributions – both direct and indirect – given by the sockets. This relies on a set of simplifying hypotheses suggested from the results of FEM simulations, and provides results in good agreement with the numerical outcomes. Although only vertical pull-out tests were considered, the above inferences are believed to apply for inclined anchors as well, since only a slight influence of the initial in situ stresses was found.

The proposed model clarifies the mechanical working conditions of the anchoring system and provides practitioners with a preliminary design framework. In the near future, further efforts will be devoted to analyse the device in the case of more complex geological conditions and, as more experimental results become available, to validate numerical/analytical predictions with respect to in situ measurements.

5 ACKNOWLEDGEMENTS

JOBSOIL s.r.l and MIDAS/GTS are gratefully acknowledged for the financial support.

6 REFERENCES

Das B.M. 1990. *Earth anchors*. Elsevier.

di Prisco C.G. and Pisanò F. 2011. An exercise on slope stability and perfect elasto-plasticity. *Géotechnique* 61 (11), 923-934.

di Prisco G.C. and Pisanò F. 2012. Numerical modelling and mechanical analysis of an innovative soil anchoring system. Submitted to *Acta Geotechnica*.

Jaeger J., Cook N.G. and Zimmermann R. 2007. *Fundamentals of rock mechanics*. Wiley-Blackwell

Merifield R.S. and Sloan S.W. 2006. The ultimate pull-out capacity in frictional soils. *Canadian Geotechnical Journal* 43 (8), 852-868.

Rowe R.K. and Davis E.H. 1982a. The behaviour of anchor plates in clay. *Géotechnique* 32 (1), 9-23.

Rowe R.K. and Davis E.H. 1982b. The behaviour of anchor plates in sand. *Géotechnique* 32 (1), 25-41.

Santoro V.M. 2009. TFEG tensioned elements: from design to implementation. *http://www.jobsoil.it/iltfeg.html* 4 (Feb 24 2009).

White D.J. Cheuk C.Y. and Bolton D. 2008. The uplift resistance of pipes and plate anchors buried in sand. *Géotechnique* 58 (10), 771-779.